A Double Negative Medium Supporting Backward Waves with Application to Microstrip Antennas

#Qun Wu [1], Ming-Feng Wu [1], Fan-Yi Meng [1], Le-Wei Li [1 2]
[1] *Department of Electrical and Communication Engineering, Harbin Institute of Technology*
Harbin 150001, China, qwu@hit.edu.cn
[2] *Department of Electrical and Computer Engineering, National University of Singapore*
Keent Ridge Crescent, Singapore 119260, LWLi@nus.edu.sg

Abstract

In this paper, a compact Double Negative (DNG) metamaterial unit cell, combined with Modified Split Ring Resonators (MSRRs) and metal strips is proposed. The Backward Wave property of the DNG slab is investigated and illustrated by full-wave simulations. It is shown that the DNG can exhibit double negative parameters and support backward wave in a broadband of 8.45 GHz~11.05 GHz range, so the existence of the DNG band is proven. Then the MSRRs and strips are stacked and embedded into a host substrate to construct a DNG substrate for the microstrip antenna (MSA) miniaturization. Results show that the presence of the DNG fillings can indeed greatly reduce the physical dimensions to 0.17λ and enhance the bandwidth of the MSA, while its farfield pattern is omnidirective, which is significantly different from that of a conventional half-wave-length MSA.

1. INTRODUCTION

Double negative medium (DNG), represents a new kind of artificially engineered electromagnetic materials by properly inserting periodic inclusions with dimensions smaller than the guided wavelength into a host material. Because DNG can exhibit negative refractive index characteristics resulted from simultaneous negative permittivity and permeability, it has been also referred to as several other names such as negative refraction index medium (NRI), left-handed material (LHM), metamaterials, and backward wave material (BWM). The basic concept of DNG was introduced by Veselago in 1968 [1], who concluded that a theoretical medium with simultaneous negative permittivity and permeability could support unusual phenomena when electromagnetic wave passed though it, including the anomalous refraction and reversal of both the Doppler effect and Cerenkov radiation. Experimentally the first effective DNG was synthesized by Smith *et al.* in microwave regime [2]. Since then, considerable attentions have been attracted to them, and remarkable progress has been achieved [3]-[8], which leads to the development of potential applications in mobile communications, medical imaging, and optoelectronics [9]–[15].

Recently, Enghata has shown that a pair of double positive medium (DPS) and DNG blocks could be used to build small resonators [16], and it has been experimentally verified [17]. Because the hybrid materials were utilized to support forward and backward waves, the phase shift gained by waves propagating in double positive medium could be compensated by waves in double negative medium. Another potential application of the above DPS-DNG phase compensator is microstrip antenna miniaturization. By theoretical analysis, several groups have found that the size of microstrip antennas can be significantly reduced by multi-pair dielectric substrates, and the dimensions of microstrip antennas could be no longer proportional to the working wavelength but approximately to the ratio of the dimensions of the dielectric blocks [18]-[20]. Although the theoretical results can be promising for microstrip antennas miniaturization, more details of research works are still necessary, especially for the practical DNG with inherent dispersion [20]-[22]. Furthermore, what is the functional mechanism of the miniaturized microstrip antenna should be more observable.

In this investigation, a compact DNG, constructed by the Modified Split Ring Resonators (MSRRs) and metal strips, is designed. It can exhibit double negative parameters and support backward waves at 8.45 GHz~11.05 GHz. Then a substrate embedded with MSRRs and strips are constructed to load a small microstrip antenna. Lastly, the small antenna is characterized and compared with conventional half-wave-length microstrip antennas to evaluate the strategy.

2. THE DNG UNIT AND THE EFFECTIVE PARAMETERS

The configuration of the DNG unit cell is shown in Fig. 1. It consists of two Modified Split Ring Resonators (MSRRs) and one strip embedded in the dielectric host medium with ε_r=2.2. The MSRR includes two square rings parallel to each other, and each ring has two gaps at opposite sides. The two rings have the same physical sizes, and the back ring (in light grey colour) is obtained by rotating the front ring (in dark grey colour) 90 degrees. The strip and the front ring (in dark grey colour) of the MSRR are on one plane. The related dimensions in Fig. 1 are: a_1=a_2= 1.78 mm, b_1=b_2=0.254 mm, c=e=0.17 mm and d=0.048 mm. The length of the strip is 2.286 mm. The sizes of the unit cell are 2.286×2.286×0.51 mm^3. The metal used here is copper.

To determine that the combination of the MSRRs and strips is indeed DNG at some frequency bands, the convenient method firstly measures the transmitted power through a sample of MSRRs alone, to identify the frequency range of the stop-band with μ<0; then measures the power transmitted through a strips alone, to identify the frequency range of the stop-band with ε<0; and finally measures the power transmitted through the composite structures [23]. If the overlapped frequency band of the two stop-bands becomes a pass-band, then it means that the combination of the MSRRs and strips is DNG at the overlapped band. Thus the microwave scattering simulation is demonstrated on the slabs with MSRRs only, strips only and both MSRRs and strips using CST MWS, respectively.

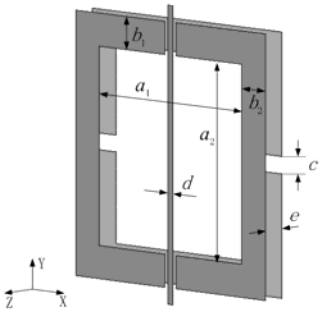

Fig. 1 Illustration of the configurations of the DNG unit cell.

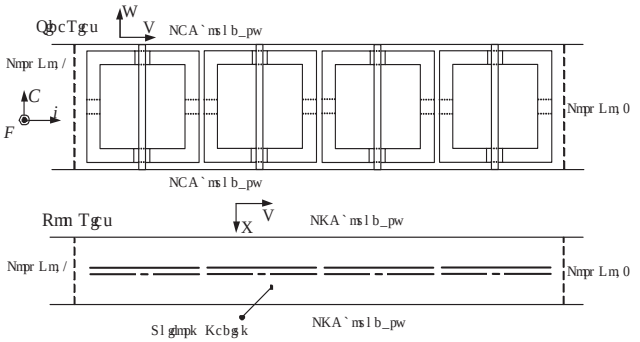

Fig. 2 Illustration of the DNG slab with 5 unit cells.

As shown in Fig. 2, the simulation configuration consists of a two-port waveguide, formed by a pair of both perfect electric conductor (PEC) and perfect magnetic conductor (PMC) walls. Five DNG units are centered in the waveguide. The incident wave is guided between the two metal plates with magnetic field in the z-direction (perpendicular to the MSRR plane) and electric field in the y-direction (along the wire). The TEM wave is transmitted from port 1 to port 2. The S_{21} magnitudes of the slabs with MSRRs only, strip only, and both the MSRRs and strips are shown in Fig. 3.

The line marked with circles represents the magnitude of S_{21} for the slab with MSRRs only, the line marked with triangles represents the magnitude of S_{21} for the slab with strips only, and the line marked with dark points represents the magnitude of S_{21} for the slab with both MSRRs and strips. It is shown that the electromagnetic wave is attenuated within 8.45 GHz~11.05 GHz for the slabs with either MSRRs only or strips only. But when it comes to the slab with both MSRRs and strips, the overlapped frequency band becomes a pass-band within about 8.45 GHz~11.05 GHz.

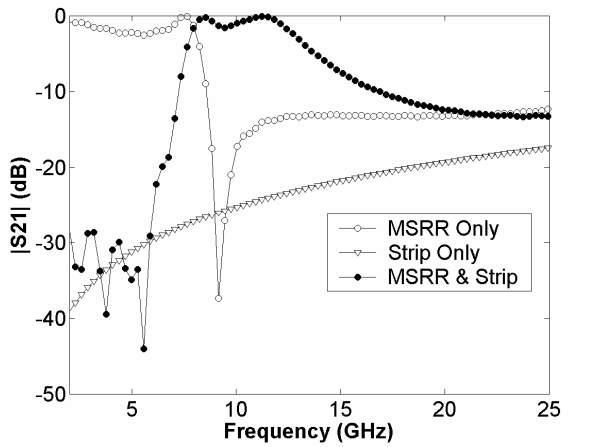

Fig. 3 Illustration of the S_{21} magnitudes of the slabs with MSRRs only, strips only, and both the MSRRs and strips.

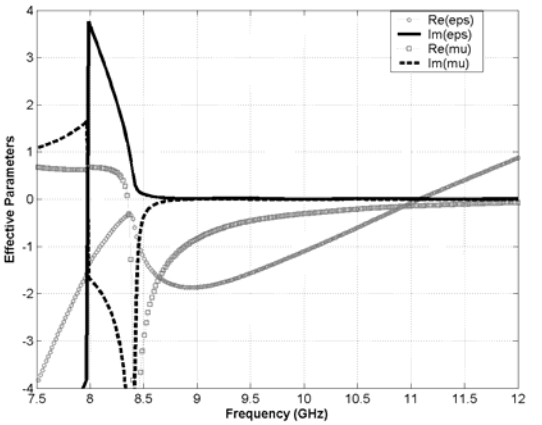

Fig. 4 Illustration of the retrieved effective parameters of the DNG

However, the pass-band is not a conclusive evidence of the existence of a DNG, so that the effective parameters ε_{DNG} and μ_{DNG} are extracted to confirm the presence from scattering parameters by the approach presented in [24] based on effective medium theory. The variations of the effective permittivity ε_{DNG} and permeability μ_{DNG} are demonstrated in Fig. 4. In Fig. 4, the solid gray line marked with circles illustrates the real part of the effective ε_{DNG}, the solid black line illustrates the imaginary part of the effective ε_{DNG}, the solid gray line marked with squares illustrates the real part of the effective μ_{DNG}, and the solid black dash line illustrates the imaginary part of the effective μ_{DNG}. It shows that the negative rang of ε_{DNG} is at 7.5-11.05 GHz, and the negative

bands of μ_{DNG} is located at 8.45-11.75 GHz. Hence, the unit cell can exhibit DNG properties over 8.45-11.05 GHz according to the retrieve approach.

3. THE BACKWARD WAVE PROPERTY OF THE DNG SLAB

One of the most interesting unusual behaviors of the DNG is the backward wave characteristic, but it is difficult to obtain and observe, especially for the practical DNG unit cell. In this part we will investigate and demonstrate the ability of the DNG slab of supporting backward waves. The simulation configuration of the DNG slab is shown in Fig. 5. 6 DNG unit cells are centered in the left part of the waveguide, and the right part of the waveguide is the same dielectric medium as the host medium of the DNG. The two-port waveguide is formed by a pair of both perfect electric conductor (PEC) and perfect magnetic conductor (PMC) walls too, which are described in Fig. 2. When the incident wave propagates from left DNG slab to right normal dielectric medium along +x-direction, with magnetic field perpendicular to the MSRR plane and electric field along the wire, we obtain the distribution of electric field in the waveguide at 8.45 GHz~11.05 GHz. The simulated E-field magnitude of the 6-cell DNG slab at 10 GHz is illustrated by the snapshots of the contour representation in Fig. 5.

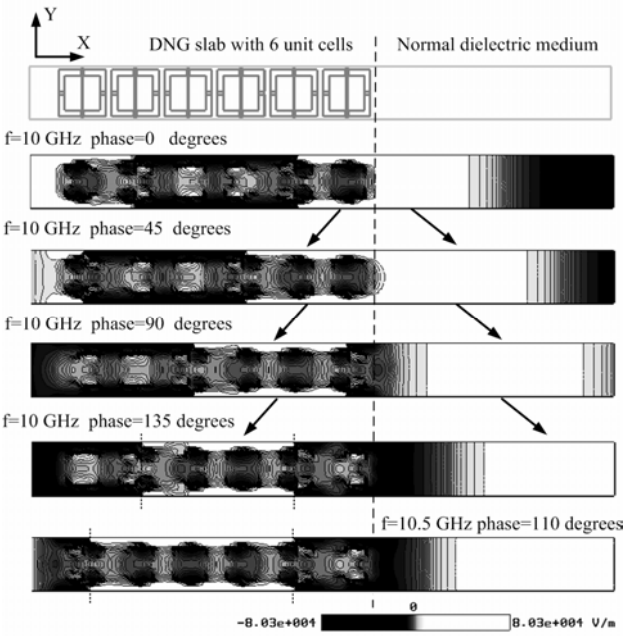

Fig. 5 Illustration of the backward wave property of the DNG slab

The phase of the excitation source at 10.0 GHz is stepped through 0, 45, 90, and 135 degrees. The field is launched in the +x-direction, and the wave front propagates along +x-direction in the right normal dielectric medium of the waveguide, but the wave front in the left DNG slab propagates toward the source, which verifies that the wave appears to move in the opposite direction as energy flow in DNG slab. Additionally, the contour of the E-field magnitude at 10.5 GHz is also depicted in Fig. 5 for comparison. It is quite evident that the distance between the neighboring nulls of the half-wavelength E-field becomes larger when the frequency is increased. With the field distributions in the DNG, it is found that the phase and group velocities are antiparallel, and the wavelength is proportional to the operating frequency.

4. THE MINIATURIZED MICROSTRIP ANTENNA

The microstrip antenna loaded by the substrate embedded with MSRRs and strips is illustrated in Fig. 6. The dimensions of the patch are W_1 in x-direction and W_2 in z-direction. The length of the microstrip feedline is L_f and the width is W_f. The dimensions of the substrate are $(D_1+W_1+W_f)$ in x-direction and $(2D_2+W_2)$ in z-direction, and the high of the substrate is H. For the filling DNG, 5 unit cells are used along the z-direction and 1 unit cell is used along the x-direction. The 5×1 DNG cells are just put under the patch to leave the two equal ends of the patch free, so we can treat the two ends the same as traditional microstrip antennas. L_R represents the length of the patch loaded by DPS in each end, while L_L represents the length of patch loaded by DNG slabs, and they sum to be the patch length L. The DPS is normal dielectric material with relative permittivity of 2.2, which is the same with the host dielectric material of the DNG slabs.

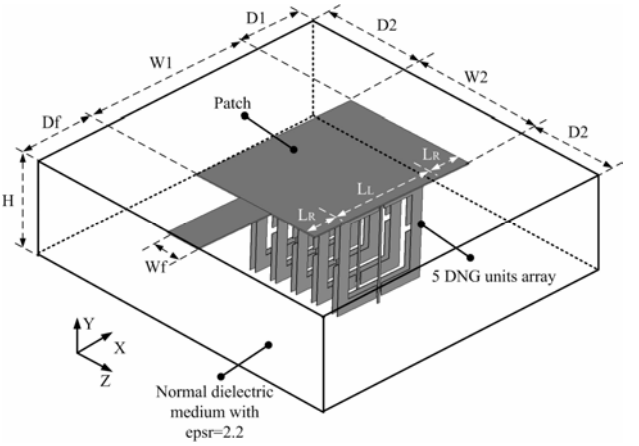

Fig. 6 Illustration of the configuration of the small microstrip antenna

Because the DNG band is located at 8.45-11.05 GHz, we choose the 9 GHz as the working frequency. The geometry parameters are as follows: D_1=1.52 mm, D_2=1.34 mm, W_1=3.81 mm, W_2=2.92 mm, H=2.29 mm, L_f=0.76 mm, D_f=1.78 mm, L_R=0.89 mm, L_L=2.03 mm. The geometric length of the patch is 3.81 mm, about 0.17λ (λ means the working wavelength of 9GHz in the host medium with ε_r=2.2), which is greatly smaller than the 0.5λ limitation.

Calculating the input admittance and the reflection coefficient for the microstrip antenna with DNG fillings, we can study the effects of the phase compensation for the waves under the patch on the antenna dimensions and performance. We can model the small patch partially loaded by DNG fillings by the Modified Transmission Line Model (MTLM), proposed in [20]. The feed of the antenna is assumed to match the antenna at 9 GHz here. By embedded the effective parameters into the MTLM, the reflection coefficient got from MTLM prediction is illustrated in Fig. 7 represented by the solid line. The reflection coefficient abruptly drops to below -20 dB at 8.50 GHz and tardily goes up at about 10.08 GHz. Although the coefficient fluctuates in the band, it shows that the small microstrip antenna can radiate well with good input admittance. The relative bandwidth is about 17.56%.

For verification, the full-wave simulation is also conducted to the small antenna with DNG fillings by CST MWS. Under above situation, the reflection coefficient got from simulation is illustrated in Fig. 7 too, represented by the dash line. Good agreement is demonstrated between the theoretical result and the full-wave simulation. So conclusions can be obtain that the DNG fillings has significantly reduced the patch length to 0.17λ, while the bandwidth has been improved to 17.56%, considering that the bandwidth of the conventional patch is about 5%. From the simulation, we note that the coefficient at 10.40-11.05 GHz is not as good as that at 8.50-10.40 GHz, although the DNG fillings still support backward waves. One factor is that the backward wave wavelengths become larger when the operating frequency increases, which has been demonstrated in the Backward Wave Property Section, so the DNG fillings shift fewer phases.

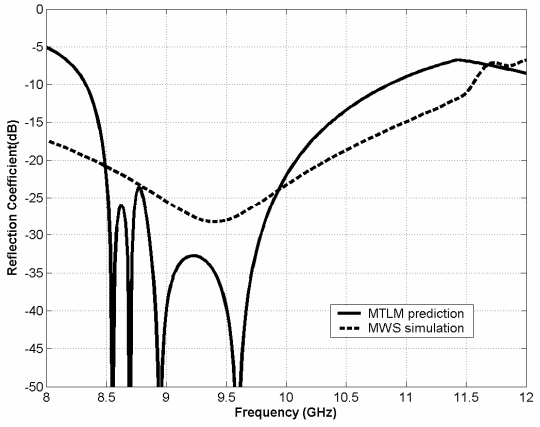

Fig. 7 Illustration of the reflection coefficient obtained from TL model and 3D full-wave simulation.

5. THE NEARFIELD AND FARFIELD OF THE SMALL MICROSTRIP ANTENNA

Furthermore, to explore the functional mechanism of the DNG fillings, the E-field distributions of the small microstrip antennas with/without DNG slabs are illustrated in Fig. 8 for comparison. It shows that when the fields on the feedline encounter the abrupt change in width at the feedline to the patch, they spread out (only electric fields are shown in the figure). This creates fringing fields at the edge, as indicated in the figure. After this transition, the patch looks like another microstrip line. The fields propagate down this transmission line until the other edge is reached. Here the abrupt ending of the line again creates fringing fields for the open-end discontinuity. The fringing fields store energy and the edges function as capacitors to ground. Because the patch is much wider than the microstrip feedline, the fringing fields also radiate, which is represented by a conductance in shunt with the edge capacitance [25].

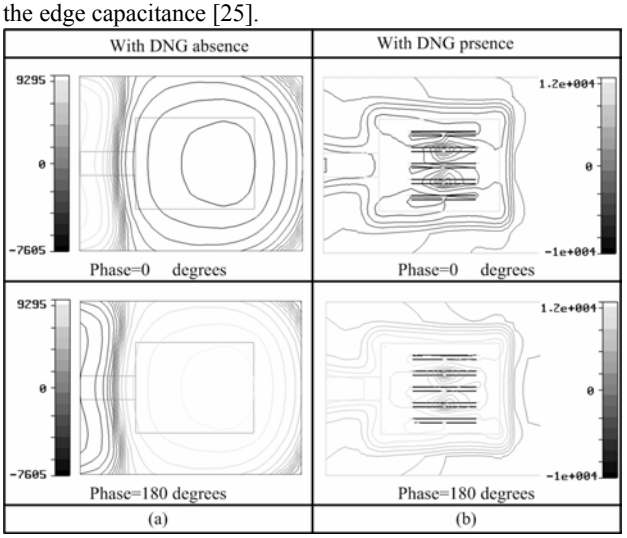

Fig. 8 Comparison of the E-field distributions between the two small microstrip antennas (a) the small path with DNG substrate absence (b) the small path with DNG substrate presence.

However, there is indeed some significant difference of the E-field fringing fields between the antennas with/without DNG slabs. For the antenna without DNG slabs shown in Fig. 8(a), the fringing fields are very intensive at the first edge, but very weak at the second edge of the patch. The reason is that the wave crest located at the first edge will come down when it reach the second edge because of the phase shift gained by waves propagating along the patch. So the fringing fields are very weak and have little radiation. When it comes to the antenna with DNG slabs shown in Fig. 8(b), the fringing fields are very intensive at both edges. Because the phase shift gained by waves propagating along the patch is compensated by the DNG slabs, which makes the fields peak value at both edges. Hence, the small antenna with DNG slabs has good radiation at both edges.

We also Note that the fringing fields distributed at the two radioactive edges are always anti-phase in conventional half-wave-length microstrip antennas, but they are almost in-phase for the patch with DNG fillings. The difference is very important, and leads to a totally different farfield pattern from traditional cases. The farfield patterns of a conventional half-wave-length patch and the patch with DNG slabs are

demonstrated in Fig. 9. Fig. 9(a) illustrates the farfield pattern of the conventional half-wave-length patch without DNG slabs working at 9 GHz loaded by normal dielectric medium with ε_r=2.2. In the pattern, 0^0 is broadside and near 90^0 is very weak. Fig. 9(b) illustrates the farfield pattern of the miniaturized microstrip antenna with DNG slabs at 9 GHz. In the pattern, near 90^0 is the broadside and 0^0 is very weak. From the comparison, it indicates that the conventional half-wave-length microstrip antenna is directive with the main lobe perpendicular to the patch, but the miniaturized microstrip antenna with DNG fillings is omnidirective.

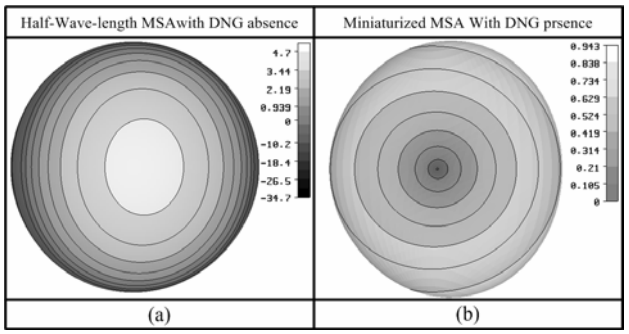

Fig. 9 Comparison of the farfield patterns between the conventional half-wave-length MSA and the miniaturized MSA with DNG presence (a) the pattern of the conventional MSA (b) the pattern of the small path with DNG substrate presence.

6. CONCLUSION

In this paper, a compact DNG, which is constructed by the Modified Split Ring Resonators (MSRRs) and metal strips, is designed with CST Microwave Studio (MWS) simulation tools. The transmission data (S_{21}) are given for the scattering of the normally incident plane wave from the DNG with MSRRs only, strips only, and both MSRRs and strips, respectively. It is shown that there is a pass-band only for the DNG with both MSRRs and strips within 8.45 GHz~11.05 GHz. Then the backward wave property of a DNG slab with periodic DNG unit cells is investigated. The full-wave simulation results show that the DNG can exhibit the backward wave phenomenon within 8.45 GHz~11.05 GHz. So the existence of the DNG is proven. Furthermore, it is quite evident that the effective wavelength of the backward wave propagating in the DNG slab becomes larger when the frequency is increased. Finally, a substrate combined by 1 DNG and two DPS blocks is designed to miniaturize the microstrip antennas (MSAs). The DNG block is filled with stacked DNG units, while the DPS blocks are normal dielectric. Later, a MSA loaded by the DNG-DPS substrate is modeled and characterized. Results show that the dimensions of the MSA have been significantly reduced to 0.17λ, and the bandwidth is enhanced to 17.56% compared to the conventional half-wave-length MSA. One of the most interesting results is that the farfield pattern is definitely different from that of conventional MSAs, i.e. the MSA with DNG substrate is omnidirective, while conventional MSAs are directive. To study the mechanism, the E-field distributions are illustrated, compared and discussed.

ACKNOWLEDGEMENT

The authors would like to express their sincere gratitude to CST Ltd. Germany, for providing various supports in using the CST MWS software to the investigation. This work was supported by the Natural Science Foundation of China under Grant 60571026, and the grant from National Key Laboratory of Electromagnetic Environment under Grant 514860303.

REFERENCES

[1] V. G. Veselago, "The electrodynamics of substances with simultaneously negative values of ε and μ," *Sov. Phys. Usp.*, vol. 10, no.4, pp.509–514, 1968.

[2] D. R. Smith, Willie J. Padilla, D. C. Vier, S. C. Nemat-Nasser, and S. Schultz, "Composite medium with simultaneously negative permeability and permittivity," *Phys. Rev. Lett.*, vol. 84, pp. 4184-4187, May 2000.

[3] R. A. Shelby, D. R. Smith, and S. Schultz, "Experimental verification of a negative index of refraction," *Science*, vol. 292, pp. 77–79, Apr. 6, 2001.

[4] A. Grbic and G. V. Eleftheriades, "Experimental verification of backward- wave radiation from a negative refractive index metamaterial," *J. Appl. Phsy.*, vol. 92, pp. 5930–5935, Nov. 2002.

[5] T. J. Yen, W. J. Padilla, N. Fang, D. C. Vier, D. R. Smith, J. B. Pendry, D. N. Basov, and X. Zhang, "Terahertz magnetic response from artificial materials," *Science*, vol. 303, pp. 1494–1496, Mar., 5 2004.

[6] G. V. Eleftheriades, A.K Iyer, and P. C. Kremer, "Planar negative refractive index media using periodically L-C loaded transmission lines," *IEEE Transactions on Microwave Theory and Techniques*, vol. 50, no. 12, pp.2702-2712, 2002.

[7] A. Sanada, C. Caloz, and T. Itoh, "Planar distributed structures with negative refractive index," *IEEE Transactions on Microwave Theory Techniques*, vol. 52, no. 4, pp.1252–1263, 2004.

[8] D. R. Smith, J. B. Pendry, and M. C. K. Wiltshire, "Metamaterials and negative refractive index," *Science*, vol. 305, pp. 788–792, Aug., 17, 2004.

[9] C. Caloz and T. Itoh, "Application of the transmission line theory of left-handed (LH) materials to the realization of a microstrip "LH line"," in *Proc. IEEE International Symp. Antennas and Propagation*, vol. 2, June 16–21, 2002, pp. 412–415.

[10] K. Buell, H. Mosallaei, and H. K. Sarabandi, "Embedded circuit magnetic metamaterial substrate performance for patch antennas," in *Proc. IEEE AP-S Int. Symp.*, vol. 2, Jun. 2004, pp. 1415–1418.

[11] A. Erentok, P. Luljak, and R.W. Ziolkowski, "Characterization of a volumetric metamaterial

realization of an artificial magnetic conductor for antenna applications," *IEEE Trans. Antennas Propag.*, vol. 53, no. 1, pp.160–172, Jan. 2005.

[12] R. W. Ziolkowski and A. D. Kipple, "Application of double negative materials to increase the power radiated by electrically small antennas," in *IEEE AP-S Int. Symp.*, vol. 51, Oct. 2003, pp. 2626–2640.

[13] A. Alu and N. Engheta, "Guided modes in a waveguide filled with a pair of single-negative (SNG), double-negative (DNG), and/or double positive (DPS) layers," *IEEE Trans. Microw. Theory Tech.*, vol. 52, pp.199–210, Jan. 2004.

[14] S.-G. Mao and S.-L. Chen, "Characterization and Modeling of Left-Handed Microstrip Lines with Application to Loop Antennas," *IEEE Transactions on Antennas and Propagations*, vol. 54, no.4, pp.1084-1091, 2004.

[15] S.-G. Mao, S.-L. Chen, and C.-W. Huang, "Effective electromagnetic parameters of novel distributed left-handed microstrip lines," *IEEE Trans. Microw. Theory Tech.*, vol. 52, no. 4, pp. 1515–1521, Apr. 2005.

[16] N. Engheta, "An idea for thin subwavelength cavity resonators using metamaterials with negative permittivity and permeability," *IEEE Antennas and Wireless Propagation Letters*, vol. 1, pp. 10-13, 2002.

[17] Y. Li, L. Ran, H. Chen, J. Huangfu, X. Zhang, K. Chen, T.M. Grzegorczyk, and J.A. Kong, "Experimental realization of a one-dimension LHM-RHM Resonator," *IEEE Transactions on Microwave Theory and Techniques*, vol. 53, no. 4, pp.1522-1526, 2005.

[18] S.F. Mahmoud, "New miniaturized annular ring patch resonator partially loaded by a metamaterial ring with negative permeability and permittivity," *IEEE Antennas and Wireless Propagation Letters*, vol. 3, pp. 19-22, 2004.

[19] W. Xu, L.-W. Li, H.-Y. Yao, T.-S. Yeo and Q. Wu, "Left-handed material effects on wave's modes and resonant frequencies: field waveguide structures and substrate-loaded patch antennas," *Journal of Electromagnetic Waves and Applications,* vol. 19, no. 15, pp. 2033-2047, October, 2005.

[20] S. A. Tretyakov and M. Ermutlu, "Modeling of Patch antennas partially loaded with dispersive backward-wave materials," *IEEE Antennas and Wireless Propagation Letters*, vol. 4, pp. 266-269, 2005.

[21] Kevin Buell, Hossein Mosallaei, and Kamal Sarabandi, "A Substrate for Small Patch Antennas Providing Tunable Miniaturization Factors," *IEEE Transactions on Microwave Theory and Techniques*, vol. 54, no. 1, pp.135, 2006.

[22] Ming-Feng Wu, Qun Wu, Fan-Yi Meng, and Jian Wu, "Investigation on the Miniaturization of the Microstrip Antenna Based on the Backward Wave Property of Left-Handed Medium," Acta. Physica. Sinica. Vol. 55, No.12, 2006, in press.

[23] A. F. Starr, P. M. Rye, D. R. Smith, and S. Nemat-Nasser, "Fabrication and characterization of a negative-refractive-index composite metamaterial," *Physical Review B*, vol. 70, pp. 113102-1-113102-4, 2004.

[24] R. W. Ziolkowski, "Design, fabrication, and testing of double negative metamaterials," *IEEE Transactions on Antennas and Propagation*, vol. 51, no. 7, pp. 1516-1529, 2003.

[25] R. Garg, P. Bhartia, I. Bahl and A. Ittipiboon, *Microstrip Antenna Design Handbook*. Norwood, MA: Artech House, 2001, sec.5.2.